J. Biomechanics Vol. 18, No. 5, pp. 307–316, 1985.
Printed in Great Britain

0021–9290/85 $3.00 + .00

KNEE FLEXOR MOMENTS DURING PROPULSION IN CYCLING—A CREATIVE SOLUTION TO LOMBARD'S PARADOX

R. J. GREGOR

Biomechanics Laboratory, Department of Kinesiology, University of California, Los Angeles, CA, U.S.A.

and

P. R. CAVANAGH and M. LAFORTUNE

Biomechanics Laboratory, The Pennsylvania State University, PA, U.S.A.

Abstract—The function of two joint muscles in the human lower extremity was studied during a cycling task with efficiency of their action discussed in light of Lombard's Paradox. Special pedals were designed to monitor reaction forces parallel to the sagittal plane of the body. Net moments of force about the hip, knee and ankle and EMG patterns in selected lower extremity muscles were recorded in five subjects pedalling against a constant load. The most original aspect of this study was the clear difference in hip and knee action during the propulsive phase of the pedalling cycle. A knee flexor moment was consistently observed in all subjects starting approximately half way through the propulsive phase of crank rotation (0–180°) and presented as a creative solution to Lombard's Paradox.

INTRODUCTION

The presence of multi-joint muscles in human and animal limbs has been suggested by some authors to involve a potential for increased efficiency (Elftman, 1966). Yet muscles spanning two or more joints may also have the potential for decreased efficiency compared to their single joint counterparts. This could occur when the required actions in a particular movement involving the joints spanned by the muscle are not those that the two-joint muscle is capable of producing. The activity of a two-joint muscle when the required moment at one of the joints is in the opposite direction to that caused by the muscle has been called Lombard's Paradox (Lombard, 1903).*

The usual example of Lombard's Paradox that is given involves standing from a chair, where it has been shown electromyographically that the two-joint members of both the hamstrings and quadriceps are active throughout the movement. The implication of this finding is that the hip extensor moment of the hamstrings (and other active hip extensors) dominates over the hip flexor action of the rectus femoris (and other active hip flexors). At the knee the reverse is true—the extensor moment of the quadriceps must be larger than the knee flexor moment of the hamstrings resulting in a net extensor moment. Clearly the activation of the two-joint muscles in this situation involves additional energy expenditure since the opposing groups work against each other at each joint. The co-contraction must be necessary to perform other functions such as stabilization of the joints.

At first sight, it might appear that the propulsive actions in cycling are another example of Lombard's Paradox. A reasonable hypothesis concerning the mechanics of propulsion is that an extensor thrust, similar to that which occurs in other locomotor activities, results from the presence of simultaneous net hip and knee extensor moments. This action would probably involve the simultaneous activity of both hamstrings and quadriceps. Such a hypothesis remains, however, unproven.

Although cycling is a commonly used form of laboratory exercise and one of the most popular recreational sports in the world, studies documenting the integrative kinetics between rider and bicycle are sparse. A review of the literature shows an enormous amount of evidence on the physiological aspects of cycling. Emphasis has been placed on utilizing the bicycle ergometer to answer questions that, for the most part, are unrelated to cycling mechanics. Glycogen depletion patterns (Gollnick *et al.*, 1974), mechanical efficiency of fast and slow fiber types (Suzuki, 1979), and EMG and oxygen uptake (Bigland-Ritchie and Woods, 1974 and Goto *et al.*, 1975) are but a few examples of physiological investigations employing a cycling task.

Houtz and Fisher (1959) utilized a laboratory ergometer and electromyography to describe the activity pattern of selected muscles in the lower extremity during the pedalling cycle. These investigators were primarily interested in the range of leg motion and the phasic action of muscles during rehabilitation. Despires (1974) and Gregor *et al.* (1982) also studied

Received 6 *June* 1984; *in revised form* 14 *August* 1984.

*It should be noted that Lombard actually identified a somewhat different musculoskeletal problem to be paradoxical.

EMG patterns during riding on a standard road racing bicycle. Gregor *et al.* had their subjects maintain a constant load, while Despires studied the effects of changes in load and seat height. Both studies report co-contraction of quadriceps and hamstrings during the power phase of the pedalling cycle. Additionally, Suzuki (1979) studied EMG at selected constant pedalling velocities but reported alternating activity in biceps femoris and rectus femoris. In light of some differences reported in EMG patterns then it would seem important to interpret EMG recordings in the context of the mechanical conditions at the time of measurement and in the case of cycling this implies that details of the forces between the foot and the pedal and of the movements of the limbs should be known.

In a classical early study Sharp (1896) used a spring dynamometer to measure the loads normal (perpendicular) to the pedal surface while subjects rode an 'ordinary' bicycle. In more recent studies many investigators have used more sophisticated instrumentation to measure either the torque applied to the crank (Daly and Cavanagh, 1976; Sargent and Davies, 1977; Sargent *et al.*, 1978) or the forces applied to the pedals (Hoes *et al.*, 1968; Dal Monte *et al.*, 1973; Gregor, 1976; Miller, 1976; Soden and Adeyefa, 1979; LaFortune and Cavanagh, 1983; Hull and Davis, 1981; Davis and Hull, 1981). Miller also measured EMG but did not report joint moments while Gregor calculated joint torques but did not record EMGs.

Only limited data on the motion of the limbs during cycling is available in the literature. Fenn (1932) used cinematography to collect data on joint motion during cycling and calculated the energy levels of the various limb segments. Nordeen and Cavanagh (1976) presented a kinematic simulation of lower limb action during cycling but neither these investigators nor Fenn used their data to calculate joint moments.

It is clear from this brief review of the literature that a complete description of the action of the lower limb during cycling remains to be presented. While the individual components of EMG and force application patterns, kinematic and kinetic descriptions have all been presented individually, an integrated description of the same subjects has not been given. It is the purpose of this paper to attempt such a description as a means of providing insight into the mechanics of the lower limb action during bicycle riding.

METHODS

Subjects

Five male subjects (mean height = 1.79 m ($\pm$0.06m), mean weight = 751 N ($\pm$23 N)) in good physical condition participated in this experiment. All were recreational cyclists and each was advised of the minimal risk involved in the testing procedure prior to participation.

Instrumentation

Forces between the feet and the pedals in a plane parallel to the sagittal plane of the body were measured by dynamometric pedals on both left and right sides of the bicycle. The left pedal is shown in Fig. 1. These special pedals actually weighed twice as much as conventional ones and only the pedal rails and bearings were standard components. The remainder of the parts were custom machined to provide surfaces for the application of strain gauges. The force cube at the center (Fig. 1, point A) permitted measurement of force components perpendicular to the pedal (called normal force, F_n) while beams near the serrated edges (Fig. 1, point B) permitted the measurement of force components parallel to the pedal surface (called tangential force, F_t). Four foil strain guages were bonded to the surface of the cube (two on the upper surface—Fig. 1, point C—and two on the lower) and connected to a fully active Wheatstone bridge amplifier. Two strain gauges were placed on each of the beams (Fig. 1, point D) and again configured in a four active arm bridge. No force by-pass to the pedal spindle was possible other than by transmission through the strain gauged members and all forces applied to the pedal were considered to resolve at the pedal spindle. Cross sensitivity between force components was measured as less than 5%. Force components parallel to the pedal spindle were not measured by this system. Each pedal was calibrated through a range of 0–1000 N in the normal direction and 0–250 N in the direction parallel to the pedal surface.

When the pedals were mounted on the bicycle (Fig. 2) pedal position with respect to the crank was monitored continuously by means of a 360° potentiometer (Fig. 2, point A), and crank angle with respect to the bicycle was monitored by a similar device (Fig. 2, point B). An infra-red LED switch emitted a pulse each time the left pedal passed through top dead center (TDC). A total of 11 analog channels were sampled by the analog to digital converter of a PDP 11/34 computer at a rate of 200 Hz per channel.

A conventional racing bicycle was mounted on a fixture designed to stimulate both the resistance and inertia that the cyclist experiences during road riding. This was achieved by a combination of frictional and electromagnetic resistance and flywheels mounted on a shaft driven from the rear tire. The actual power output of the rider was calculated directly from the force and position data subsequent to the ride. This yields a more accurate estimate of power output than an ergometer setting since losses in the ergometer are included in the present measurement. All analog data were averaged over 50 pedal revolutions during each trial to provide an average response that was used in subsequent calculations.

Body segment parameters

Calculation of joint torques required that estimates be made of selected segment parameters for the thigh, shank and foot on the left side of the body. In order to personalize the data for each subject, segment masses were calculated using the regression equations presented by Clauser *et al.* (1969). Segmental moments of

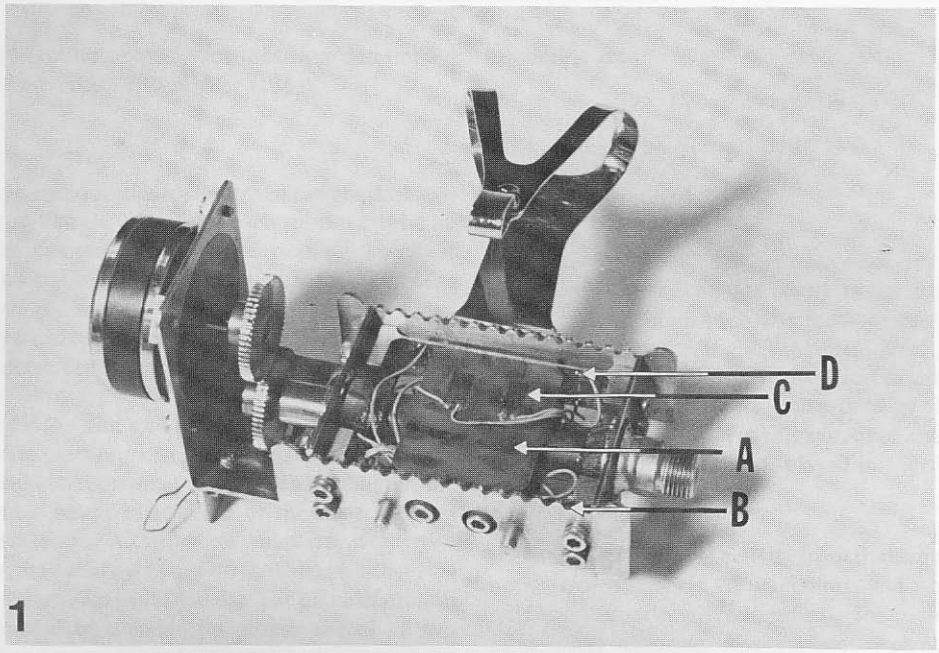

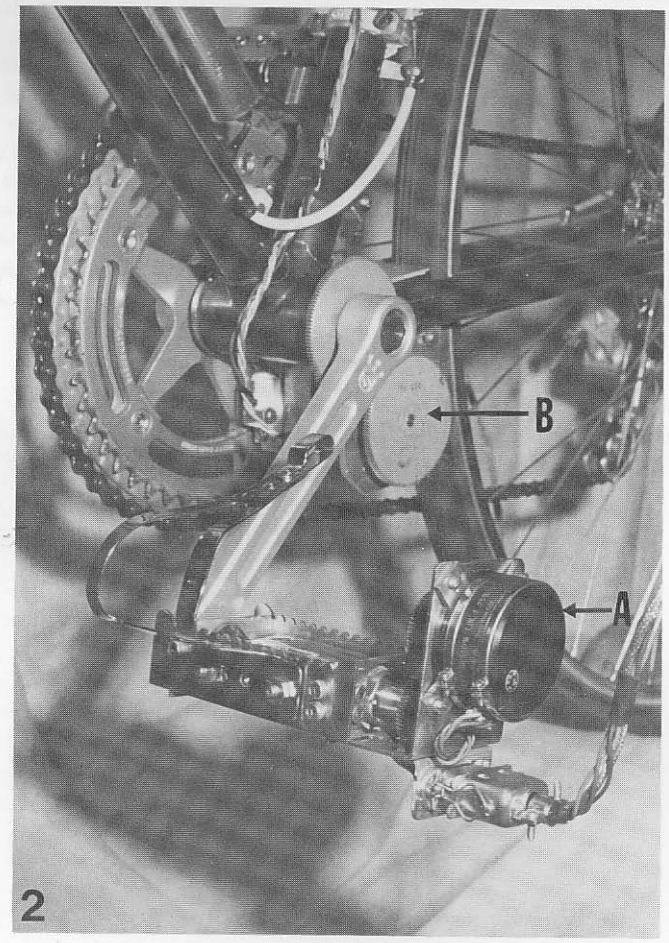

Fig. 1. Bicycle pedal designed to measure reaction force components. Point A indicates the center cube designed to measure the force component perpendicular (F_n) to the pedal surface. Point C illustrates two of the four strain gauges applied to the cube. Point B indicates the serrated edges designed to measure the force component parallel to the pedal surface (F_t). Point D illustrates one of the four gauges applied to the two edges.

Fig. 2. The left pedal mounted on the bicycle. Point A indicates the potentiometer designed to monitor pedal orientation with respect to the crank and Point B illustrates the potentiometer used to monitor crank angle.

Note: Page 310 is blank (backside of photos)

inertial and center of mass locations were determined using the methods of Dempster (1955).

Cinematography analysis

One high speed 16 mm motor driven camera (LoCam) was used to film the left side of each subject during all trials. The camera operated at a nominal speed of 100 frames s^{-1} and was oriented with the film plane parallel to the sagittal plane. Internal timing lights driven by a quartz crystal generator served to calibrate camera speed. The output from the TDC indicator was displayed in the field of view of the camera to synchronize the film and force data.

Reflective markers were applied to the skin overlying the superior border of the greater trochanter, the approximate center of rotation of the knee, and the lateral malleolus. Contrasting markers were also placed on the heel, two points on the shoe on either side of the pedal and the pedal spindle. The plane of motion was calibrated by means of a plumb line of known length filmed in the field of view which also provided a vertical reference for subsequent digitization.

A Vanguard motion analyzer and Hewlett-Packard Digitizer/Calculator System (HP Model 9830A) were employed to extract necessary data points from the film. The coordinates of the hip, knee, ankle, foot and pedal markers from two consecutive pedalling cycles were digitized and smoothed by means of a digital filter (7 Hz cutoff) and second derivatives were calculated by means of a moving window second degree least square polynomial (Lanczos, 1957).

Equations of motion

All body segments were assumed to be rigid bodies and conventional Newtonian mechanics were used to derive equations of motion. The three equilibrium equations are

$$F_X - m\mathrm{d}^2 x/\mathrm{d}t^2 = 0$$

$$F_Y - m\mathrm{d}^2 y/\mathrm{d}t^2 = 0$$

$$\Upsilon - I_p \mathrm{d}^2\theta/\mathrm{d}t^2 = 0$$

where m = mass, I_P = segmental moment of inertia about the proximal end of the segment, $\mathrm{d}^2x/\mathrm{d}t^2$ = acceleration of the mass center in the x direction, $\mathrm{d}^2y/\mathrm{d}t^2$ = acceleration of the mass center in the y direction, $\mathrm{d}^2\theta/\mathrm{d}t^2$ = angular acceleration, F_X and F_Y = the net horizontal and vertical forces on the segment. An inertial reference frame fixed in the experimental bicycle was used in this system of analysis and reference conventions are displayed in Fig. 3.

EMG

Patterns of electrical activity from the semimembranosus, biceps femoris, rectus femoris and vastus lateralis were monitored continuously for each subject. Silver/silver chloride disc surface electrodes with adhesive collars were placed 2.5 cm apart over the belly of the muscle.

AC wide band differential amplifiers conditioned the signals which were then stored on FM tape. Interference patterns (EMG) were subsequently digitized off line at a rate of 833 Hz, full wave rectified and integrated over 15° sections of the pedal revolution. The magnitude of the integral in the segment with the largest integrated EMG was designated 100% and the integrals in all other segments were expressed with respect to that reference (% max).

Protocol

Test protocol required each rider to pedal at 60 RPM for four minutes with a power output of approximately 160 W. Toe clips and cleated shoes were

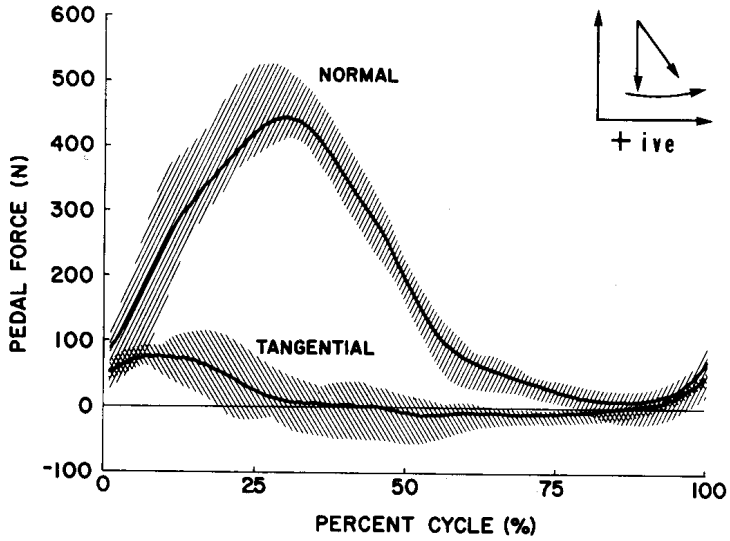

Fig. 3. Mean normal (F_n) and shear (F_t) reaction force patterns for five subjects. Shaded area represents the range of values across the five subjects with five cycles for each subject (25 total cycles). Sign convention used in analysis is illustrated in the upper right hand corner.

worn by all subjects and all data were collected during the last minute of each ride.

RESULTS

Pedal reaction forces

Mean reaction force patterns representing the response of this group of subjects to a constant workload setting at 60 RPM are graphically displayed in Fig. 3. (Note that the forces applied to the pedal by the rider are of the same magnitude but in the opposite direction.) Force values from the left side have been shifted by 180° to generate the average response from both legs. The force curves are shown as functions of cycle time (where 100% represents one complete revolution). These mean patterns represent averages of 500 pedalling cycles (50 revolutions × 2 legs × 5 riders). The shaded areas indicate the range of values measured from the five subjects for both right and left sides. Positive F_n indicates pushing down normal to the pedal surface and a positive F_t indicates pushing forward along the surface of the pedal.

The normal force component (F_n) rose to a peak value of 445 N at 108° into the pedalling cycle and then declined rapidly to 193 N by 180° and only 26 N at 270°. It should be noted that small but positive forces were recorded during the recovery phase of the revolution. The peak value of the tangential component (78 N at 36°) was less than 20% of the peak normal force. F_t fell approximately to zero by 120° after TDC and remained near zero for the major portion of the pedal revolution.

The important output from the rider as far as propulsion is concerned is the effect of these forces in the production of a resultant moment about the crank. This pattern, for one leg, shown in Fig. 4, indicates a rapid rise to a fairly steady level between 90 degrees and 120 degrees. A decline is then observed as the crank approaches bottom dead center with torques around zero for the remainder of the pedalling cycle.

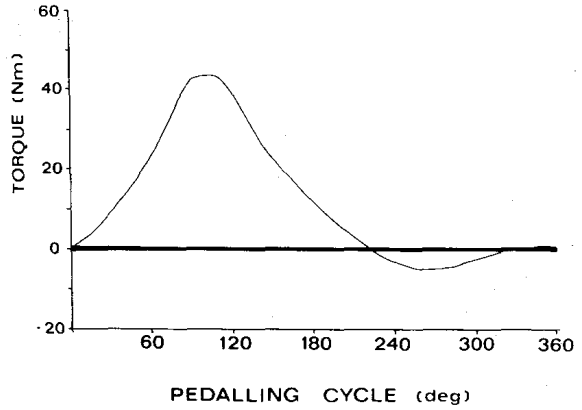

Fig. 4. Resultant moment about the crank for the left leg in all subjects.

Joint moment patterns

Mean torque patterns representing the response of this group of subjects to a constant workload are displayed in Fig. 5. Net torque about the ankle was found to be plantar flexor (negative) for the first 200° of the revolution and close to zero for the remainder of the cycle. The curve is extremely similar to the normal force curve and examination of the terms in the equation shows F_n to be the major component in the ankle torque calculation. The peak torque of −55 Nm was attained at approximately 102° into the pedalling cycle near the same time peak F_n was recorded. The variation between subjects was relatively small as seen by the shaded range in Fig. 5.

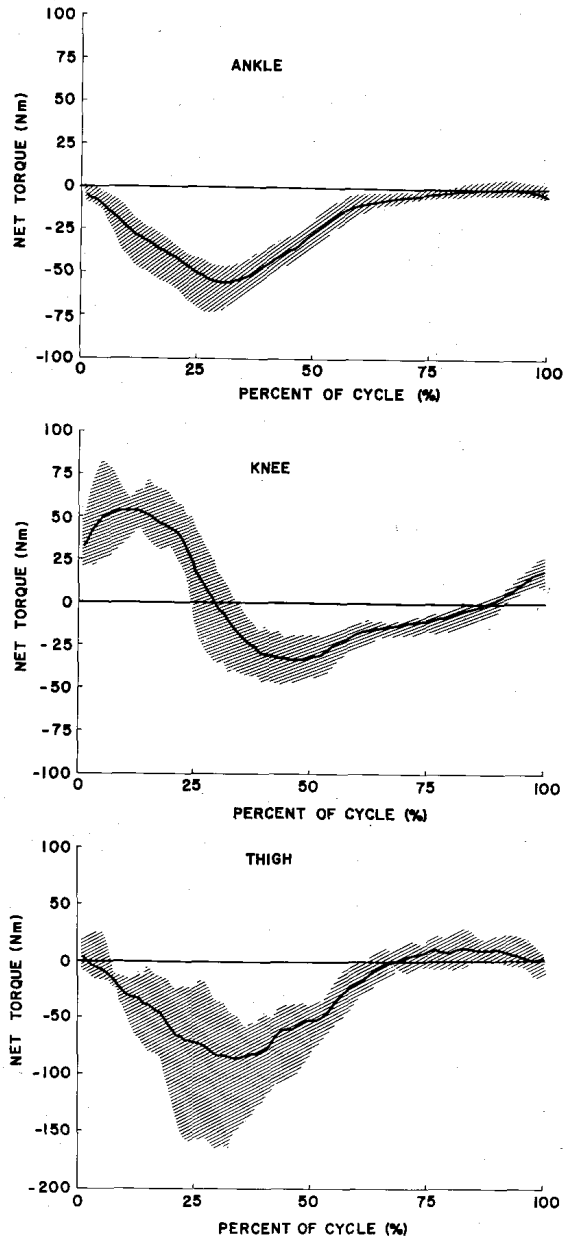

Fig. 5. Mean joint torque patterns about the ankle, knee, hip, (thigh) for five subjects. Shaded area represents the range of values across two pedalling cycles for each subject (ten total cycles).

Knee moments also displayed a fairly consistent pattern in this group of five subjects. A knee extensor (positive) torque was found during the initial 29% of the pedalling cycle with a peak of 53 Nm occurring at only 36° from TDC (Fig. 5b). The net joint moment then reversed and a peak knee flexor moment at −34 Nm (range −20 Nm to −46 Nm) occurred just before BDC (mean angle 154°). This flexor moment continued until 325° at which point it became positive again increasing in magnitude through top dead center. Some variation in the timing of the first extensor peak was noted but the general pattern was similar in all subjects with the moment always reversing from extensor to flexor between 88° and 123°.

Like the ankle joint torques, hip torques were found to be extensor for most of the pedal cycle reaching a peak value of −86 Nm at 110° (Fig. 5c). Small flexor torques were observed during the final 30° of the cycle with a peak value of 12 Nm at 276°. Considerable variation in the peak extensor moments were found between subjects with a range from −63 to 166 Nm.

Muscle activity patterns

Average integrated EMG patterns for the semimembranosus, biceps femoris, rectus femoris and vastus lateralis, from four of the five subjects are illustrated in Fig. 6. The data in Fig. 6 are similar to a polar coordinate graph where the magnitude of the integral in each 15° segment is proportional to the radius of the corresponding segment of the graph. The mean angle of the segment on the graph is the mean angle from TDC at which the data were collected.

The two electrode pairs on the medial and lateral hamstrings revealed very different phasic patterns. The medial hamstring site displayed activity throughout the pedalling cycle with values greater than 50% for more than half the cycle (30–210 degrees). A plateau of activity above 80% of maximum recorded values was evident between 60 and 150°. The lateral hamstring, however, displayed a large amount of relative activity earlier in the cycle but still showed a plateau of activity greater than 75% of maximum recorded for a 120 degree segment beginning at ±15° before TDC. Thus the combined activity of the lateral and medial hamstring group was at a high level all the way from 15° before TDC until 30° after BDC.

The pattern of activity from the two electrode sites over the quadriceps showed very different patterns from each other. The electrode pair overlying rectus femoris experienced its greatest activity just prior to top dead center with activity above 50% of the maximum recorded values occurring for a fairly brief

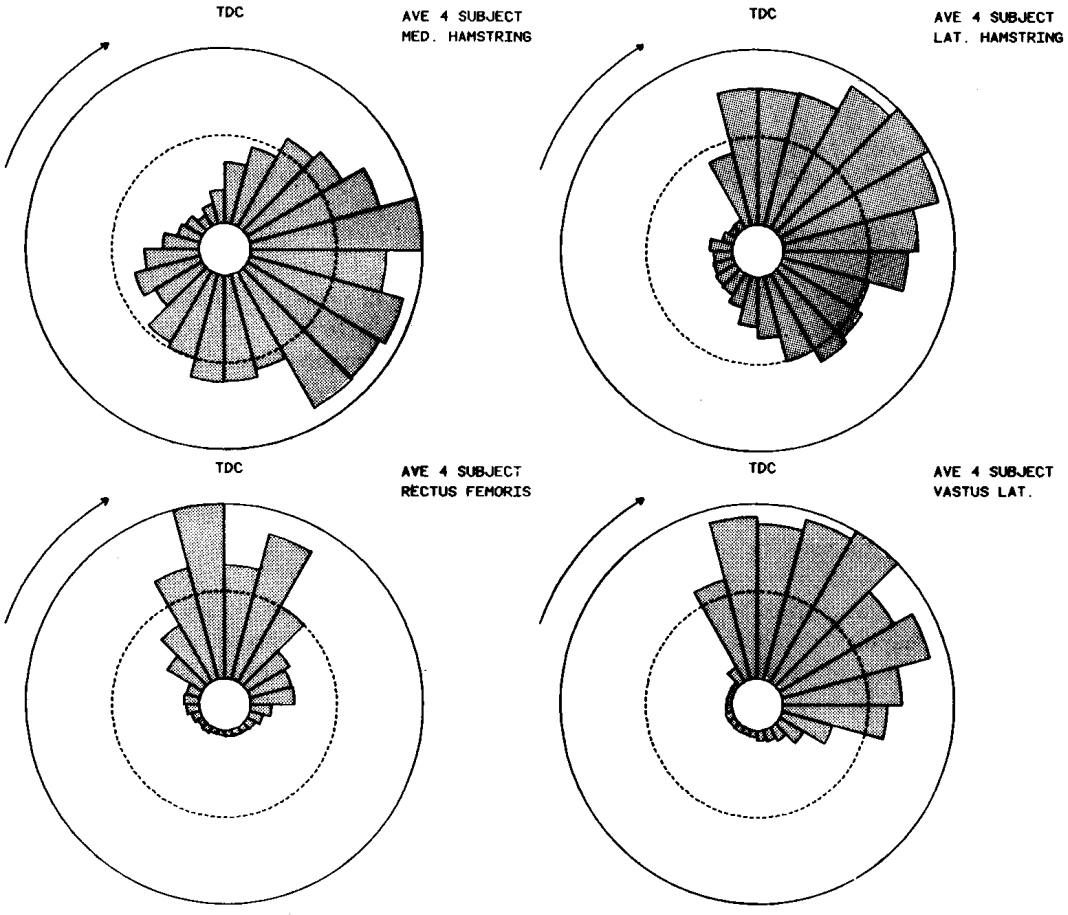

Fig. 6. Average integrated EMG patterns for the medial hamstring, lateral hamstring, rectus femoris and vastus lateralis. Each shaded section reprsents per cent of maximum activity over 15° of the pedalling cycle in four of the five subjects. The dashed line represents 50 percent of maximum activity observed in that muscle.

period between 30° before TDC to 30° after. Activity at the electrode site overlying vastus lateralis showed a longer burst of activity with values above 75% of the recorded maximum beginning 15° before TDC until 75° after TDC. In contrast to the medial hamstring pattern, both quadriceps sites showed minimal activity between major bursts for a sector of at least 225°.

It should be noted that the activity at the quadriceps electrode sites is always accompanied by activity at the hamstring locations. Thus there is always co-contraction of knee flexors and extensors during periods of extensor activity.

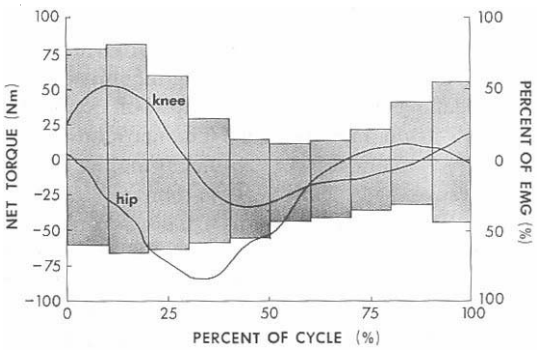

Fig. 7. Mean joint torque patterns for the hip and knee (Fig. 3) and average EMG (%max) pattern using data from Fig. 4 and Gregor *et al.* (1982). Mean patterns for VL, VM and RF are above the 0 % line while mean patterns for BF, SM, GM are below the 0 % line.

DISCUSSION

When the joint moments are examined in relation to the crank moment during propulsion, it is clear that the hip and knee are very different in their actions. During this phase the moment at the hip is always extensor. The knee moment however is first extensor and then flexor (see Fig. 5). These patterns were consistent over all subjects.

This observation and its explanation represent the most original aspects of this study. It should be noted that it is theoretically possible to ride a bicycle employing extensor moments at the knee throughout the propulsive phase. However, to do so would be a direct example of Lombard's Paradox. The knee extensor muscles would have to develop moments in excess of the flexor moment generated at the knee by the two joint hip extensors. This, as discussed earlier, would be an extremely uneconomical situation metabolically.

An examination of the EMG data alone from this and previous studies (Gregor, 1982) would have given some indication of the findings related to knee joint action. EMG at the qualitative level offers an on/off judgement that, in this case, allows us to state that the absence of major knee extensor activity in the second quadrant implies that the active extensor moment is small.

On the quantitative level the limitations of estimating muscle moments from EMG are well known. Such factors as muscle length, velocity and moment arm differences related to joint position prevent the establishment of clear relationships between EMG and joint moments (Chapman and Calvert, 1979). It is nevertheless instructive to compare the quantified EMG with joint moment data and this has been done in Fig. 7. In this figure the EMG data above the zero percent line represents an average of the data presented in Fig. 6 and that presented by Gregor *et al.* (1982) for the vastus lateralis, vastus medialis and rectus femoris. EMG data below the zero percent line represents average activity patterns for the gluteus maximus, semimembranosus and biceps femoris from this study and that by Gregor *et al.* (1982). This combination of EMG and torques suggests the dominance of knee extensors over hip extensors which also act at the knee during the early part of the propulsive phase. In the second quadrant, the substantial reduction of knee extensor EMG activity illustrates the lack of co-contraction of the flexors and extensors in the production of flexor moments at the knee and extensor moments at the hip.

When both the joint moments and the EMG data are considered together, the advantage of the combination of data over a consideration of either one singly is apparent. If only resultant moments were available and they were, for example, net flexor moments at the knee we would be unable to distinguish between the case where there was only hamstring activity and the case where hamstring activity was dominant over coactive quadriceps activity. If, however, only EMG activity were available, and there was, for example, co-contraction of flexors and extensors, the factors mentioned earlier would prevent the establishment of the relative dominance of the two groups in the production of a resultant joint moment. In the current context, we have been able to show that the combination of joint moments and pattern of muscle activity indicate the avoidance of the consequences of Lombard's Paradox at the knee joint during the second half of the propulsion phase during cycling.

The finding of knee flexor moments during propulsion is somewhat counter-intuitive. The most direct way to confirm this finding is to draw the resultant force vector in its spatial relationship to the leg at a time when the moment is negative (flexor). This has been done in Fig. 8 where it is apparent that the force vector passes in front of the knee joint and therefore produced a moment tending to extend the knee. This is resisted by a muscular moment that tends to flex the knee. The fact that the knee joint is still extending (see Fig. 9) during this phase might lead us to believe that the resultant moment is necessarily extensor. One need only consider the action of slowly lowering a weight held in the hand to encounter a more common example of a net flexor moment at a joint which is extending. The results of the present paper are an interesting example of a pattern of activation of the musculature where external forces are applied in what would appear

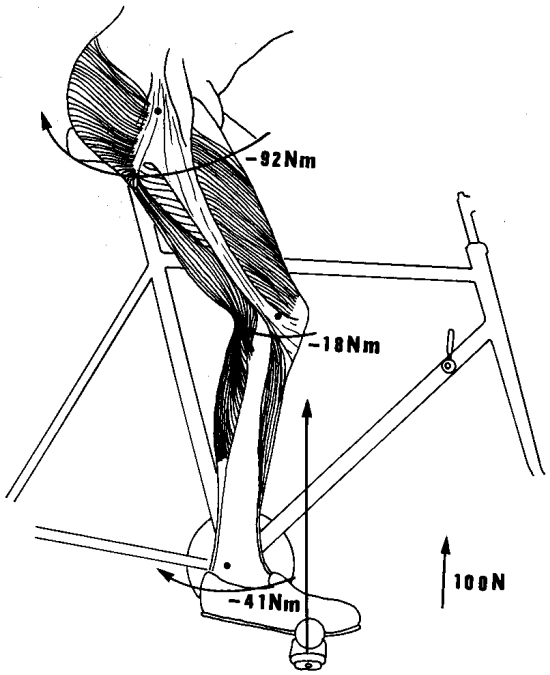

Fig. 8. Schematic of the right lower extremity of one subject at 135° in the pedalling cycle. Curved arrows represent the direction of the calculated torque and the straight arrow indicates the resultant pedal reaction force.

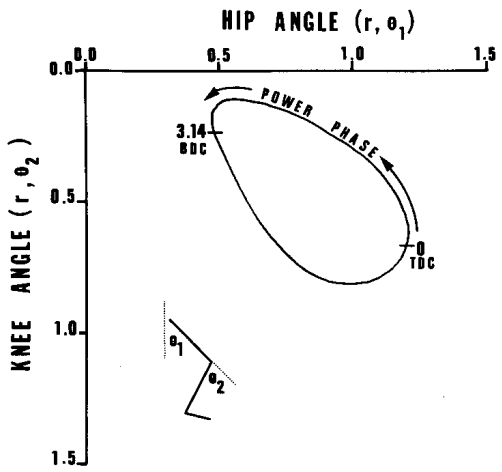

Fig. 9. Angle/angle diagram for the hip and knee for this group of five subjects during one pedalling cycle. The power phase is indicated from 0r (top dead center) to 3.14 (180° on bottom dead center). Angle convention is in the lower left corner of the figure.

to be a creative solution to the probelms posed in Lombard's Paradox.

REFERENCES

Bigland-Ritchie, B. and Woods, J. J. (1974) Integrated EMG and oxygen uptake during dynamic contractions of human muscles. *J. appl. Physiol.* **36,** 475–479.

Chapman, A. C. and Calvert, T. W. (1979) Estimation of active state from EMG recordings in human muscular contraction. *Electromyograph. clin. Neurophys.* **19,** 199–222.

Clauser, C. E., McConville, J. T. and Young, J. W. (1969) Weight volume and centre of mass of segments of the human body. AMRL-TR—69–70. Aerospace Medical Research Laboratories, Wright-Patterson Air Force Base, OH.

Dal Monte, A., Manoni, A. and Fucci, S. (1973) Biomechanical study of competitive cycling. *Biomechanics III* (Edited by Cerquiglini, S., Venerando, A. and Wartenweiler, J.), pp. 434–439. University Park Press, Baltimore.

Daly, D. J. and Cavanagh, P. R. (1976) Asymmetry in bicycle ergometer pedalling. *Med. Sci. Sports* **8,** 204–208.

Davis, R. R. and Hull, M. L. (1981) Measurement of pedal loading in bicycling—II. Analysis and Results. *J. Biomechanics* **14,** 857–872.

Dempster, W. (1955) Space requirements of the seated operator. USAF, WADC, Technical Report 55–159. Wright Patterson Air Force Base, Ohio.

Despires, M. (1974) An electromyographic study of competitive road cycling conditions simulated on a treadmill. *Biomechanics IV* (Edited by Nelson, R. C. and Morehouse, C. A.), pp. 349–355. University Park Press, Baltimore.

Elftman, H. (1966) Biomechanics of muscle with particular application to studies of gait. *J. Bone Jt Surg.* **48A,** 363–377.

Fenn, W. O. (1932) Zur Mechanik des Radfahrens in Vergleich zu der des Laufens. *Pflügers Arch. ges. Phsiol.* 229–354.

Gregor, R. J. (1976) A biomechanical analysis of lower limb action during cycling at four different loads. Unpublished Doctoral dissertation, Pennsylvania State University, University Park, PA.

Gregor, R. J., Green, D. and Garhammer, J. J. (1982) An electromyographic analysis of selected muscle activity in elite competitive cyclists. *Biomechanics VII-B.* (Edited by Morecki, A., Fidelus, K., Kedzior, K. and Wit, A.) pp. 537–541. University Park Press, Baltimore.

Gollnick, P. D., Piehl, K. and Saltin, B. (1974) Selective glycogen depletion patterns in human muscle fibers after exercise of varying intensity and at varying pedalling rates. *J. Physiol.* **241,** 45–57.

Goto, S., Toyoshima, S. and Hoshikawa, T. (1975) Study of the integrated EMG of leg muscles during pedalling at various loads, frequency and equivalent power. *Biomechanics V-A.* (Edited by Komi, P.) pp. 246–252. University Park Press, Baltimore.

Hoes, M. J. A. J. M., Binkhorst, R. A., Smeekes-Kuyl, A. E. M. C. and Vissers, A. C. A. (1968) Measurement of forces exerted on pedal and crank during work on a bicycle ergometer at different loads. *Int. Z. angew. Physiol.* **26,** 33–42.

Houtz, S. A. and Fischer, F. J. (1959) An analysis of muscle action and joint excursion during exercise on a stationary bicycle. *J. Bone Jt. Surg.* **41–A,** 123–131.

Hull, M. L. and R. R. Davis (1981) Measurement of pedal loading in bicycling—I. Instrumentation. *J. Biomechanics* **14,** 843–856.

La Fortune, M. A. and Cavanagh, P. R. (1983) Effectiveness and efficiency during bicycle riding. *Biomechanics VIIIB* (Edited by Matsui, H. and Kobayashi, K.), pp. 928–936. Human Kinetics Publishers, Champaign, IL.

Lanczos, C. (1957) *Applied Analysis.* Pitmans, New York.

Lombard, W. P. (1903) The action of two-joint muscles. *Am. Phys. Ed. Rev.* **8,** 141–145.

Miller, N. (1976) The effect of load, speed and configuration on the electromyographic activities of the skeletal muscles. Unpublished Doctoral Dissertation, Univeristy of Wisconsin-Madison.

Nordeen, K. S. and Cavanagh, P. R. (1976) Simulation of lower limb kinematics during cycling. *Biomechanics V-B.* (Edited by Komi, P. V.), pp. 26–33. University Park Press, Baltimore.

Sargent, A. J., Charters, A., Davies, C. T. M. and Reeves, E. S.

(1978) Measurement of forces applied and work performed in pedalling a stationary bicycle ergometer. *Ergonomics* **21,** 49–53.

Sargent, A. J. and Davies, C. T. M. (1977) Forces applied to cranks of a bicycle ergometer during one and two-led cycling. *J. appl. Physiol.* **42,** 514–518.

Sharp, A. (1896) *Bicycles and Tricycles*, pp. 268–270. Longmans Green (reprinted M.I.T. Press, Cambridge, 1977).

Soden, P. D. and Adeyefa, B. A. (1979) Forces applied to a bicycle during normal cycling. *J. Biomechanics* **12,** 527–541.

Suzuki, Y. (1979) Mechanical efficiency of fast and slow twitch muscle fibers in man during cycling. *J. appl. Physiol.* **47**(2), 263–267.

Suzuki, S., Watanabe, S. and Saburo, H. (1982) EMG activity and kinematics of human cycling movements at different constant velocities. *Brain Res.* **240,** 245–258.